JOURNAL OF AGRICULTURAL AND FOOD CHEMISTRY

ARTICLE

pubs.acs.org/JAFC

Study on the Binding of Propiconazole to Protein by Molecular Modeling and a Multispectroscopic Method

Chao Wang and Ying Li*

Key Laboratory of Integrated Regulation and Resource Development on Shallow Lakes of Ministry of Education, and College of Environment, Hohai University, NanJing, JiangSu Province 210098, China

ABSTRACT: Propiconazole (PCZ) is an *N*-substituted triazole used as a fungicide on fruits, grains, seeds, hardwoods, and conifers. Although the triazole fungicides have shorter half-lives and lower bioaccumulation than the organochlorine pesticides, possible detrimental effects on the aquatic ecosystem and human health also exist. To evaluate the toxicity of PCZ at the protein level, its effects on human serum albumin (HSA) were characterized by molecular modeling and multispectroscopic method. On the basis of the fluorescence spectra, PCZ exhibited remarkable fluorescence quenching, which was attributed to the formation of a complex. The thermodynamic parameters ΔH and ΔS were calculated to be −14.980 KJ/mol and 26.966 J/(mol K), respectively, according to the van't Hoff equation, which suggests hydrophobic and electrostatic interactions are the predominant intermolecular forces in stabilizing the PCZ−protein complex. Furthermore, HSA conformation was slightly altered in the presence of PCZ. These results indicated that PCZ indeed affected the conformation of HSA.

KEYWORDS: propiconazole, protein, molecular modeling, fluorescence spectroscopy

INTRODUCTION

Recently, the widespread use of pesticides in agriculture resulting in a series of toxicological and environmental problems has generated extensive concerns.[1] Because most pesticides are not completely degraded after application, their metabolites and some unchanged forms of these compounds are excreted and subsequently enter the ecosystem.[2] Propiconazole (*cis*−*trans*-1-[2-(2,4-dichlorophenyl)-4-propyl-1,3-dioxolan-2-ylmethyl]-1*H*-1,2,4-triazole, PCZ; Figure 1) is a triazole antifungal agent that is a member of the class of ergosterol biosynthesis inhibiting fungicides. PCZ is one of approximately 40 azole (imidazole or triazole) containing fungicides used in worldwide commerce. PCZ is used as a fungicide on bananas, barley, boronia, chrysanthemums, grapes, peanuts, pineapples, poppies, prunes, stone fruits, sugar cane, barley, and wheat and for the prevention and control of needle/leaf and stem fungi and powdery mildews on hardwoods and conifers.[3] Although the triazole fungicides have shorter half-lives and lower bioaccumulation than the organochlorine pesticides, possible detrimental effects on the aquatic ecosystem may arise from spray drift or surface runoff after rainfall.[4] PCZ has been listed by the European Union as a persistent and potentially toxic compound.[5,6] PCZ can exert adverse effects in mammals, fish, insects, mollusks, and zooplankton.[3,7] Humans can become exposed through runoff from treated fields or golf courses and through the air after aerosol application. Environmental exposure to PCZ tends to 0.012−12 μg/L in surface waters[8] and 0.08−0.20 mg/kg in food residues.[9] Therefore, knowledge of the interaction mechanisms between PCZ and plasma protein is of crucial importance for us to understand its possible dangers to the human body.

As the first choice, human serum albumin (HSA) is a principal extracellular protein with a high concentration in blood plasma and is a globular protein consisting of a single polypeptide chain of 585 amino acid residues, exhibiting several important physiological functions.[10] HSA considerably contributes to colloid osmotic blood pressure and serves in the transportation and distribution of many molecules and metabolites, such as fatty acids, amino acids, hormones, cations, anions, drugs, and xenobiotics.[11−13] Spectroscopic techniques have become popular methods for revealing molecule−protein interactions because of their high sensitivity, rapidity, and ease of implementation. They allow nondestructive measurements of substances in low concentration under various experimental conditions.[14−19] These techniques provide the binding information and reflect the conformation changes of proteins in various environments. However, none of the investigations determined in detail the binding mechanism, binding constants, binding mode, and effects of protein secondary structure between triazole antifungal agent and HSA. This study is designed to examine the influence of PCZ on the structure of HSA under physiological conditions to obtain more knowledge on interaction mechanisms of PCZ−HSA.

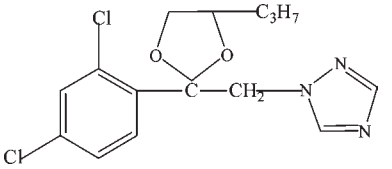

Figure 1. Chemical structure of propiconazole.

In the present work, the interaction mechanisms of PCZ−HSA were demonstrated by using molecular modeling and multispectroscopic methods. The toxicity mechanism at the protein level was predicted through molecular modeling, and the binding parameters were confirmed using a series of spectroscopic methods. Attempts were made to investigate the binding constant (K), thermodynamic parameters for the reaction, and the effect of PCZ

Received: March 12, 2011
Revised: June 24, 2011
Accepted: June 26, 2011
Published: June 26, 2011

on protein secondary structure. Furthermore, results obtained by spectroscopic methods are consistent with those of the molecular modeling study. These results provide accurate and full basic data for clarifying the binding mechanisms of PCZ with HSA in vivo and are important for food safety and human health when using triazole antifungal agent.

MATERIALS AND METHODS

Materials. Human serum albumin (70024-90-7, 98%, purity) was purchased from Sigma Chemical Co. All HSA solutions were prepared in pH 7.40 buffer solutions, and the HSA stock solution was kept in the dark at 4 °C. Propiconazole was of analytical grade purchased from Dr. Ehrenstorfer Co. (Germany), and stock solutions were prepared in absolute ethanol. NaCl (1.0 M) solution was used to maintain the ionic strength at 0.1. Buffer (pH 7.40) consists of Tris (0.2 M) and HCl (0.2 M), and the pH was adjusted to 7.40. Other reagents were of analytical grade, and deionized water was used throughout all of the experiments.

Apparatus and Methods. Fluorescence spectra were measured with an LS-50B spectrofluorophotometer (Perkin-Elmer, USA). The fluorescence excitation wavelength was 280 nm, and the emission was read at 300−500 nm. The intrinsic fluorescence of HSA was obtained at 350 nm when excited at 280 nm. A quantitative analysis of the potential interaction between PCZ and HSA was performed by fluorometric titration. A 3 mL solution containing 7.5×10^{-7} M HSA was titrated by successive additions of PCZ. Because the PCZ acceptable daily intake (ADI) is 0.04 mg/kg day and its maximum residue limit (MRL) is 5 mg/kg,[20] the experimental concentration of PCZ was 10^{-6}−10^{-5} M. The fluorescence intensity was measured (excitation at 280 nm and emission at 350 nm). All experiments were measured at four different temperatures (23, 30, 37, and 44 °C). Using the fluorescence decrease, the association constants K for the complex of PCZ with HSA at different temperatures were calculated.

Circular dichroism measurements were made on a Chriascan CD spectrometer (Applied Photophysics, U.K.), using a 2 mm cell at 23 °C. The spectra were recorded in the range of 200−260 nm, and the scan rate was 30 nm/min. The induced ellipticity of the protein alone was defined as the ellipticity of the PCZ−HSA mixture minus the ellipticity of PCZ alone at the same wavelength.

Infrared spectroscopy was recorded at room temperature using a Nicolet Nexus 670 FT-IR spectrometer (USA) equipped with a Geranium attenuated total reflection (ATR) accessory, a deuterated triglycine sulfate (DTGS) detector, and a KBr beam splitter. All infrared spectra were taken via the ATR method with a solution of 4 cm^{-1} and 128 scans. The FT-IR spectrum of free HSA was acquired by subtracting the absorption of the Tris buffer solution from the spectrum of the protein solution, and a difference spectrum of HSA was obtained by subtracting the spectrum of PCZ from that of PCZ−HSA at the same concentration.

The crystal structure of HSA in complex with R-warfarin was taken from the Brookhaven Protein Data Bank (entry code 1h9z).[21] The potential of the three-dimensional structure of HSA was assigned on the basis of the Amber 4.0 force field with Kollman-all-atom charges. The initial structure of PCZ was generated by molecular modeling software Sybyl 6.9.[22] The geometry of the molecule was subsequently optimized to minimal energy using the Tripos force field with Gasteiger−Marsili charges, and the FlexX program was used to build the interaction modes between PCZ and HSA. All calculations were performed on an SGI FUEL workstation.

RESULTS AND DISCUSSION

Analysis of Fluorescence Quenching of HSA by PCZ. Fluorescence quenching is the decrease of the quantum yield of fluorescence from a fluorophore induced by a variety of molecular interactions with a quencher molecule. HSA is a globular protein comprising 585 amino acid residues. In these amino acid residues, tryptophan, tyrosine, and phenylalanine residues are the only three intrinsic fluorophores. In fact, the intrinsic fluorescence of HSA is almost due to tryptophan alone because phenylalanine has a very low quantum yield and the fluorescence of tyrosine is almost totally quenched if it is ionized or near an amino group, a carboxyl group, or a tryptophan. This viewpoint was well supported by the experimental observations of Sulkowska.[23] In other words, the change of intrinsic fluorescence intensity of HSA was due to tryptophan residues when small molecules bound to HSA.

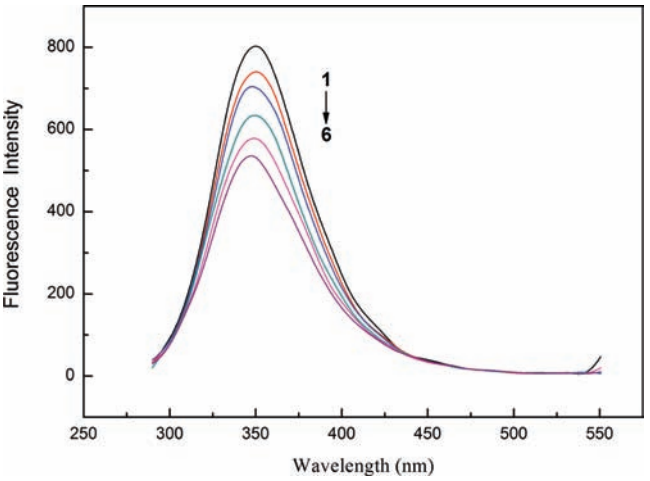

Figure 2. Fluorescence emission spectra of the PCZ−HSA system: (1) HSA; (2−6) PCZ−HSA; [HSA] = 7.5×10^{-7} M; [PCZ] = 8.2×10^{-6} and 1.6×10^{-5} M, 3.2×10^{-5}, 4.8×10^{-5}, and 6.3×10^{-5} M; λ_{ex} = 280 nm; T = 23 °C; pH 7.4.

The aim of the present work was to investigate the binding properties of PCZ to HSA. The fluorescence spectra of HSA before and after addition of PCZ were measured with the excitation wavelength at 280 nm, and their representative spectra are shown in Figure 2. The conformation changes in protein were evaluated by measuring the intrinsic fluorescence intensity of protein tryptophan residues[24] before and after the addition of PCZ. The addition of PCZ caused a dramatic decrease in the fluorescence emission intensity of HSA. It can be seen that a higher excess of PCZ led to more effective quenching of the chromophore molecules' fluorescence. These results suggested that there may be changes in the immediate environment of the tryptophan and tyrosine residues. This means that the molecular conformation of the protein was affected during its transportation and distribution in blood.

Binding Mechanism and Binding Parameters. Fluorescence quenching refers to any process that decreases the fluorescence intensity of a sample. It is divided into dynamic quenching or static quenching. Dynamic quenching depends upon diffusion. Because higher temperatures result in larger diffusion coefficients, the biomolecular quenching constants are expected to increase with increasing temperature. In contrast, increased temperature is likely to result in decreasing stability of complexes and, thus, lower values of the static quenching constants.[25]

A possible quenching mechanism is derived from the Stern−Volmer plots (Figure 3) of the system at four temperatures (23, 30, 37, and 44 °C). The classical Stern−Volmer

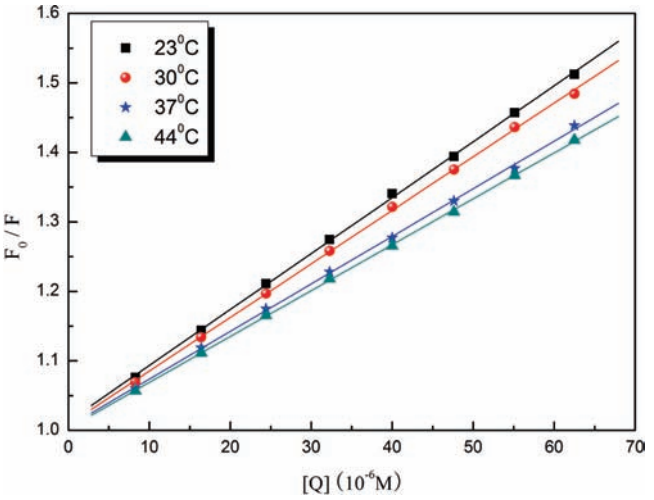

Figure 3. Stern−Volmer plots of fluorescence quenching of PCZ−HSA system. [HSA] = 7.5×10^{-7} M; [PCZ] = 8.2×10^{-6}−6.3×10^{-5} M; λ_{ex} = 280 nm, λ_{em} = 350 nm; pH 7.4.

Table 1. Dynamic Quenching Constants between PCZ and HSA

T (°C)	Stern−Volmer eq	K_Q (L/mol/s)	R
23	$Y = 1.013 + 0.00804[Q]$	8.04×10^{11}	0.9997
30	$Y = 1.00831 + 0.00771[Q]$	7.71×10^{11}	0.9997
37	$Y = 1.00551 + 0.00685[Q]$	6.86×10^{11}	0.9996
44	$Y = 1.00306 + 0.00661[Q]$	6.61×10^{11}	0.9999

equation is[26]

$$F_0/F = 1 + K_Q \tau_0[Q] = 1 + K_{SV}[Q]$$

where F_0 and F are the fluorescence intensities in the absence and presence of quencher, respectively. K_Q is the biomolecular quenching constant, τ_0 is the lifetime of the fluorescence in the absence of quencher (for most biomolecules, τ_0 is about 10^{-8} s), [Q] is the concentration of quencher, and K_{SV} is the Stern−Volmer quenching constant. The results summarized in Table 1 show that the Stern−Volmer quenching constant K_{SV} is inversely correlated with temperature and that the values of K_Q are greater than the limiting diffusion constant, K_{dif}, of the biomolecule ($K_{dif} = 2.0 \times 10^{10}$ L mol^{-1} s^{-1}).[27] This implies that the quenching mechanism does not spring from dynamic quenching but proceeds from static quenching.

The quantitative analysis of the binding of PCZ to HSA was carried out using Scatchard's procedure:[28]

$$r/D_f = nK - rK$$

This method is based on the general equation, where r is the moles of molecule bound per mole of protein, D_f is the molar concentration of free molecule, n is the binding site multiplicity per class of binding sites, and K is the equilibrium binding constant. Figure 4 shows the Scatchard plots for the system at different temperatures. The linearity of the Scatchard plot indicated that PCZ bound to a single class of binding sites on HSA and that there was an interaction between PCZ and HSA (Table 2). The binding constant decreased slightly with the increasing temperature, resulting in a reduction of the stability of the PCZ−HSA complex.

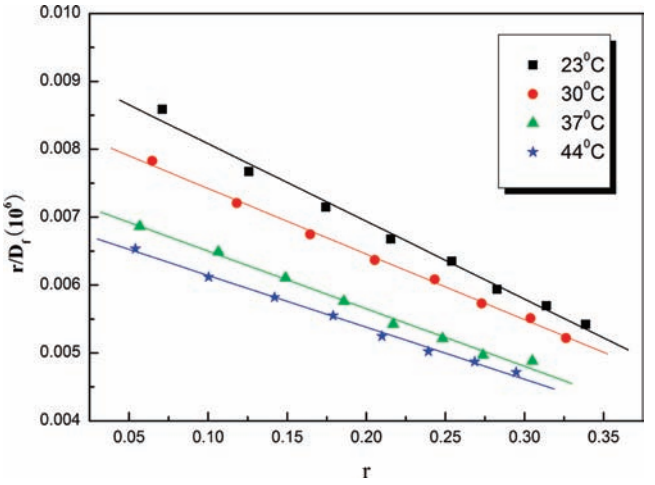

Figure 4. Scatchard curves of quenching of HSA with PCZ. [HSA] = 7.5×10^{-7} M; [PCZ] = 8.2×10^{-6}−6.3×10^{-5} M; λ_{ex} = 280 nm, λ_{em} = 350 nm; pH 7.4.

Table 2. Binding Constants between PCZ and HSA

T (°C)	Scatchard eq	K (L/mol)	R
23	$Y = 0.00923 - 0.01144r$	1.14×10^4	0.9957
30	$Y = 0.00839 - 0.00965r$	9.65×10^3	0.9985
37	$Y = 0.00735 - 0.00847r$	8.47×10^3	0.9962
44	$Y = 0.00691 - 0.00764r$	7.64×10^3	0.9978

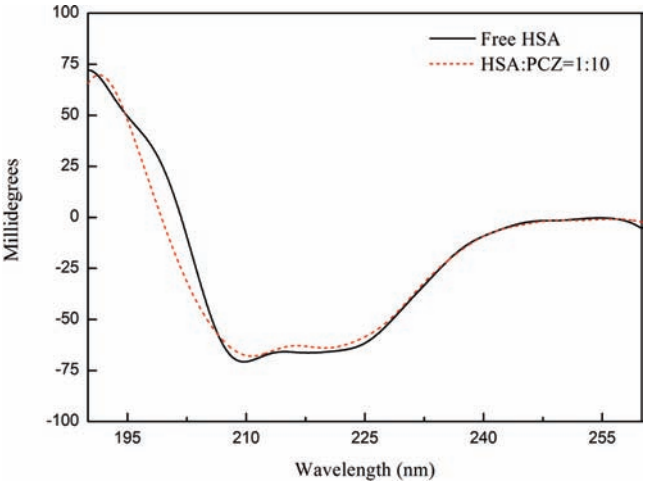

Figure 5. CD spectra of the HSA−PCZ system. [HSA] = 6.0×10^{-7} M; [PCZ] = 6.0×10^{-6} M; T = 23 °C; pH 7.4.

Changes of the Protein's Secondary Structure Induced by PCZ. CD is one of the strongest and most sensitive spectroscopic techniques used to explore the various aspects of protein structure and also to understand the interaction between protein and small molecules. To gain a better understanding of the physicochemical properties of PCZ governing its spectral behavior and to draw relevant conclusions on the PCZ−HSA binding mechanism, CD spectroscopic measurement was performed. If the change of protein structure included the transformation of protein secondary structure in the molecule−protein complex, it can be reflected in the CD spectra. The CD spectra of protein

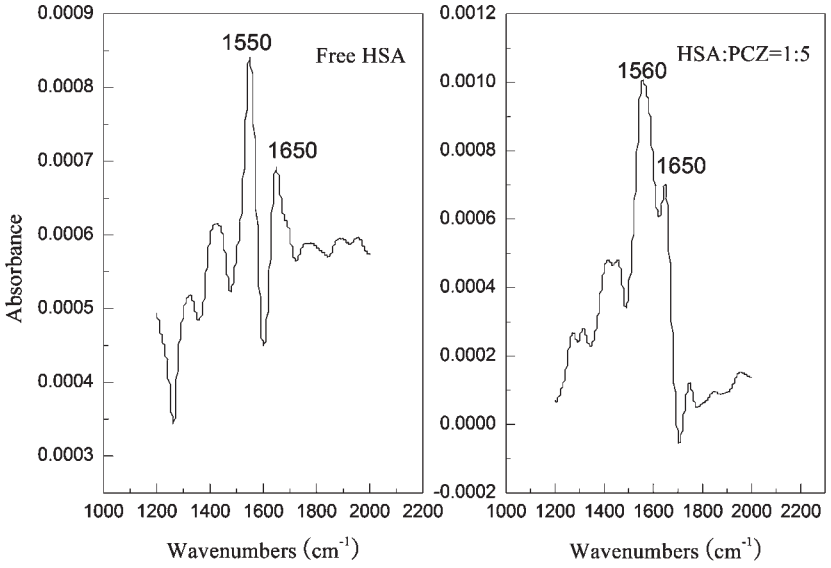

Figure 6. FT-IR spectra and difference spectra of HSA in aqueous solution. [HSA] = 6.0×10^{-7} M; [PCZ] = 3.0×10^{-6} M; T = 23 °C; pH 7.4.

consist of two negative bands in the ultraviolet region at 209 and 220 nm, which is typical characterization of the α-helix structure of this class of protein.[29] The reasonable explanation is that the negative peaks between 208 and 209 nm and between 222 and 223 nm both contributed to $n \rightarrow \pi^*$ transfer for the peptide bond of the α-helix.[30] The value in CD spectrum observed around 215 nm is characteristic of β-sheet structure.[31] Here the CD spectrum was taken in the wavelength range from 200 to 260 nm, and the results are expressed as mean residue ellipticity in millidegrees. Figure 5 shows a typical CD spectrum of HSA in the presence and absence of PCZ. The ellipticity values in the CD spectrum slightly decrease in the presence of PCZ. This indicates that the conformation change is limited and occurs only locally; that is, the protein secondary structure is slightly disturbed by PCZ.

Additional evidence regarding PCZ−HSA interactions was obtained from FT-IR spectroscopic results. The infrared spectrum of a protein exhibits a number of amide bands, which represent different vibrations of the peptide moiety. Among all amide modes of the peptide group, the amide I band ranges from 1600 to 1700 cm^{-1} and the amide II band region ranges from 1500 to 1600 cm^{-1}, and both of them are relevant to the secondary structure of the protein.[32−34] Figure 6 shows the FT-IR spectra of the free and bound forms of HSA. It can be concluded that the secondary structure of HSA is changed because the peak position of amide II was shifted from 1550 cm^{-1} (in free HSA) to 1560 cm^{-1} (in PCZ−HSA), together with the change in the peak shape. These results indicated that the PCZ has interacted with HSA and resulted in conformational changes of the secondary structure of HSA.

Binding Mode. In general, small molecules are bound to macromolecules through four binding modes: hydrogen bond, van der Waals force, and electrostatic and hydrophobic interactions. The thermodynamic parameters, the enthalpy and entropy of a reaction, are important for confirming the binding mode. For this reason, the binding constants of PCZ to HSA at four temperatures were estimated. The temperatures chosen were 23, 30, 37, and 44 °C, so that HSA does not undergo structural degradation. The thermodynamic parameters were obtained from a linear van't Hoff plot and are presented in Table 3. Nemethy and Scheraga,[35] Timasheff,[36] and Ross and Subramanian[37] characterized the sign and magnitude of the thermodynamic parameter associated with various individual kinds of interaction that might take place in the protein association processes, as described below. $\Delta H > 0$ and $\Delta S > 0$ imply a hydrophobic interaction; $\Delta H < 0$ and $\Delta S < 0$ reflect the van der Waals force or hydrogen bond formation; and $\Delta H \approx 0$ and $\Delta S > 0$ suggest an electrostatic force. As shown in Table 3, ΔH and ΔS for the binding reaction between PCZ and HSA were found to be −14.980 kJ/mol and 26.966 J/(mol K). Therefore, the binding of PCZ to HSA might involve hydrophobic interaction as verified by the positive values of ΔS, whereas the electrostatic interaction could not be excluded. That is, PCZ bound to HSA was mainly based on the hydrophobic and electrostatic interactions.

Table 3. Thermodynamic Parameters for the Binding PCZ and HSA

T (°C)	ΔG (kJ/mol)	ΔH (kJ/mol)	ΔS (J/mol K)
23	−22.961		
30	−23.150	−14.980	26.966
37	−23.339		
44	−23.528		

Molecular Modeling Studies on the Interaction between PCZ and HSA. HSA has a limited number of binding sites for endogenous and exogenous ligands that are typically bound reversibly and have binding constants in the range of 10^4−10^8 M^{-1}.[38] The principal regions of ligand binding sites of albumin are located in hydrophobic cavities in subdomains IIA and IIIA, which exhibit similar chemistry. To explore which binding site of HSA PCZ was located in, the complementary applications of molecule modeling were employed to improve the understanding of the interaction between HSA and PCZ. The crystal structure of HSA in complex with R-warfarin was taken from the Brookhaven Protein Data Bank (entry code 1h9z). The partial binding parameters of the HSA−PCZ system were calculated using an SGI FUEL workstation, and the best energy ranked result is shown in Figure 7. From Figure 7, it is important to note

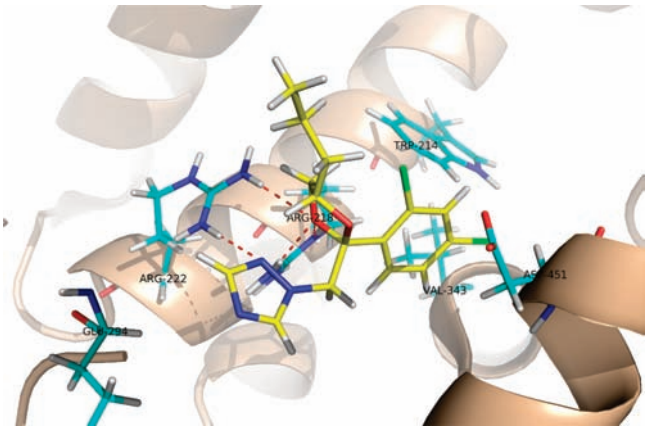

Figure 7. Best binding mode for HSA−PCZ system according to FlexX program. The secondary structure of the protein is shown, and the important neighboring amino acids are labeled. Ligand structures are shown in a ball and stick format. The hydrogen bonds are indicated by a red dash.

that PCZ is in the hydrophobic cavity of HSA. In addition, there are four hydrogen bonds between PCZ and the amino acid residues of HSA. As shown, PCZ is mainly hydrophobic and appears to form hydrogen bonds with residues Arg218 and Arg222. The interaction between PCZ and HSA is not exclusively hydrophobic in nature because there are several ionic and polar residues in the proximity of the ligand playing important roles in stabilizing the molecule via hydrogen bonding and electrostatic interaction. However, although the molecule can be docked into the binding pocket of HSA, the interaction is still very weak because the size of PCZ is small compared to that of the binding pocket. The calculated binding ΔG is −16.17 kJ/mol, which also indicates the weak interaction between HSA and PCZ.

The widespread use of PCZ (a triazole antifungal agent) in agriculture resulted in a series of toxicological and environmental problems. Knowledge of its binding to proteins contributes to the understanding of its toxicity in vivo. This work establishes the binding mode of PCZ with HSA under physiological conditions by multispectroscopic methods and molecular modeling techniques. A fluorescence method was eliminated to get accurate data (binding parameters). On the basis of the thermodynamic results, it was considered that PCZ binds to HSA through the hydrophobic and electrostatic interactions, and according to the molecular modeling study, hydrogen bonds exist between PCZ and HSA. Furthermore, the HSA model and molecular docking methods were applied to further define that PCZ interacts with the Arg218 and Arg222 residues of HSA. In addition, fluorescence, FT-IR, and CD results showed that the binding of PCZ can cause conformational and some microenvironmental changes of HSA. The work provides accurate and full basic data for clarifying the binding mechanisms of PCZ with HSA in vivo and is helpful for understanding its effect on protein function during its transportation and distribution in blood.

Funding Sources

The presented study was supported by the National Key Basic Research Development Program (973 project) of China (2010CB429006), the State Key Program of the National Natural Science Foundation of China (No. 50830304), the Scholar Climb Program of the Jiangsu Natural Science Foundation (BK2008041), and the Fundamental Research Funds for the Central Universities (No. 2009B18214).

ABBREVIATIONS USED

HSA, human serum albumin; PCZ, propiconazole; CD, circular dichroism; FT-IR, Fourier transform infrared.

REFERENCES

(1) Li, Z. H.; Randak, T. Residual pharmaceutically active compounds(PhACs)in aquatic environment — status, toxicity and kinetics: a review. *Vet. Med.* **2009**, *52*, 295–314.

(2) Fent, K.; Weston, A. A.; Caminada, D. Ecotoxicology of human pharmaceu-ticals. *Aquat. Toxicol.* **2006**, *76*, 122–159.

(3) Sun, G. B.; Thai, S. F.; Douglas, B. T.; Guy, R. L.; Amber, K. G.; Douglas, C. W.; David, J. D.; Stephen, N. Propiconazole-induced cytochrome P450 gene expression and enzymatic activities in rat and mouse liver. *Toxicol. Lett.* **2005**, *155*, 277–287.

(4) Konwick, B. J.; Garrison, A. W.; Avants, J. K.; Fisk, A. T. Bioaccumulation and biotransformation of chiral triazole fungicides in rainbow trout (*Oncorhynchus mykiss*). *Aquat. Toxicol.* **2006**, *80*, 372–381.

(5) Adam, O.; Bitschene, M.; Torri, G.; Giorgi, F. D.; Badot, P. M.; Crini, G. Studies on adsorption of propiconazole on modified carbons. *Sep. Purif. Technol.* **2005**, *46*, 11–18.

(6) Wu, Q. L.; Riise, G. H.; Kretzschmar, R. Size distribution of organic matter and associated propiconazole in agricultural runoff material. *J. Environ. Qual.* **2003**, *32*, 2200–2206.

(7) Hakoi, K.; Cabral, D. R.; Hoshiya, T.; Hasegawa, R.; Shirai, T.; Ito, D. N. Analysis of carcinogenic activity of some pesticides in a medium-term liver bioassay in the rat. *Teratogen. Carcinog. Mut.* **1992**, *12*, 269–276.

(8) Li, Z. H.; Vladimir, Z.; Li, P.; Roman, G.; Josef, V.; Jana, M.; Tomas, R. Biochemical and physiological responses in liver and muscle of rainbow trout after long-term exposure to propiconazole. *Ecotoxicol. Environ. Saf.* **2010**, *73*, 1391–1396.

(9) Torres, C. M.; Picó, Y.; Manes, J. Comparison of octadecylsilica and graphitized carbon black as materials for solid-phase extraction of fungicide and insecticide residues from fruit and vegetables. *J. Chromatogr., A* **1997**, *778*, 127–127.

(10) Dugiaczyk, A.; Law, S. W.; Dennison, O. E. Nucleotide sequence and the encoded amino acids of human serum albumin Mrna. *Proc. Natl. Acad. Sci. U.S.A.* **1982**, *79*, 71–75.

(11) Liu, J. Q.; Tian, J. N.; Li, Y.; Yao, X. J.; Hu, Z. D.; Chen, X. G. Binding of the bioactive component daphnetin to human serum albumin demonstrated using tryptophan fluorescence quenching. *Macromol. Biosci.* **2004**, *4*, 520–525.

(12) Li, Y.; Yao, X. J.; Jin, J.; Chen, X. G.; Hu, Z. D. Interaction of rhein with human serum albumin investigation by optical spectroscopic technique and modeling studies. *Biochim. Biophy. Acta — Proteins Proteomics* **2007**, *1774*, 51–58.

(13) Wang, Q.; Zhang, Y. H.; Sun, H. J.; Chen, H. L.; Chen, X. G. Study of interaction of butyl-*p*-hydroxy benzoate with human serum albumin by molecular modeling and multi-spectroscopic method. *J. Lumin.* **2011**, *131*, 206–211.

(14) Shankara, S. K.; Jaldappagari, S.; Umesha, Ka. Voltammetric and spectroscopic investigations on the mechanism of interaction of buzepide methiodide with protein. *Colloids Surf. B.* **2010**, *75*, 75–79.

(15) Li, Y.; Wang, C.; Lu, G. H. Interaction of jatrorrhizine with human γ-globulin in membrane mimetic environments: probing of the binding mechanism and binding site by spectroscopic and molecular modeling methods. *J. Mol. Struct.* **2010**, *980*, 108–113.

(16) Liu, X. P.; Du, Y. X. Study on the binding of chiral drug duloxetine hydrochloride to human serum albumin. *Eur. J. Med. Chem.* **2010**, *45*, 4043–4049.

(17) Yuan, J. L.; lv, Z. Liu, Z. G.; Hu, Z.; Zou, G. L. Study on interaction between apigenin and human serum albumin by spectroscopy

and molecular modeling. *J. Photochem. Photobiol. A: Chem.* **2007**, *191*, 104–113.

(18) Xiao, J.; Suzuki, M.; Jiang, X.; Chen, X.; Yamamoto, K.; Ren, F.; Xu, M. Influence of B-ring hydroxylation on interactions of flavonols with bovine serum albumin. *J. Agric. Food Chem.* **2008**, *56*, 2350–2356.

(19) Tian, J. N.; Liu, J. Q.; Hu, Z. D.; Chen, X. G. Interaction of wogonin with bovine serum albumin. *Bioorg. Med. Chem.* **2005**, *13*, 4124–4129.

(20) Bert, R.; Pieter, S.; Geert, H.; Betty, H.; Sofie, I.; Walter, S. Quantitative determination of the influence of adjuvants on foliar fungicide residues. *Crop Prot.* **2007**, *26*, 1589–1594.

(21) Petitpas, I.; Bhattacharya, A. A.; Twine, S.; East, M.; Curry, S. Crystal structure analysis of warfarin binding to human serum albumin. *J. Biol. Chem.* **2001**, *276*, 22804–22809.

(22) Morris, G. SYBYL software, version 6.9, Tripos Associates, St. Louis, MO, 2002.

(23) Sulkowska, A. Interaction of drugs with bovine and human serum albumin. *J. Mol. Struct.* **2002**, *614*, 227–232.

(24) Yuan, T.; Weljie, A. M.; Vogel, H. J. Tryptophan fluorescence quenching by methionine and selenomethionine residues of calmodulin: orientation of peptide and protein binding. *Biochemistry* **1998**, *37*, 3187–3195.

(25) Lu, Y.; Feng, Q. Q.; Cui, F. L.; Xing, W. W.; Zhang, G. S.; Yao, X. J. Interaction of 30-azido-30-deamino daunorubicin with human serum albumin: investigation by fluorescence spectroscopy and molecular modeling methods. *Bioorg. Med. Chem. Lett.* **2010**, *20*, 6899–6904.

(26) Eftink, M. R. Fluorescence quenching reactions: probing biological macromolecular structures. In *Biophysical and Biochemical Aspects of Fluorescence Spectroscopy*; Dewey, T. G., Ed.; Plenum Press: New York, 1991.

(27) Lakowica, J. R.; Weber, G. Quenching of fluorescence by oxygen. Probe for structural fluctuations in macromolecules. *Biochemistry* **1973**, *12*, 4161–4170.

(28) Scatchard, G. The attractions of protein for small molecules and ions. *Ann. N.Y. Acad. Sci.* **1949**, *51*, 660–673.

(29) Trynda-Lemiesz, L.; Karaczyn, A.; Keppler, B. K.; Koztowski, H. Studies on the interactions between human serum albumin and transindazolium (bisindazole) tetrachlororuthenate(III). *J. Inorg. Biochem.* **2000**, *78*, 341–346.

(30) Yang, P.; Gao, F. *The Principle of Bioinorganic Chemistry*; Science Press: Beijing, China, 2002; p349.

(31) He, W. Y.; Li, Y.; Tang, J. H.; Luan, F.; Jin, J.; Hu, Z. D. Comparison of the characterization on binding of alpinetin and cardamonin to lysozyme by spectroscopic methods. *Int. J. Biol. Macromol.* **2007**, *39*, 165–173.

(32) Wi, S.; Pancoka, P.; Keiderling, T. A. Predictions of protein secondary structures using factor analysis on Fourier transform infrared spectra: effect of Fourier self-deconvolution of the amide I and amide II bands. *Biospectroscopy* **1998**, *4*, 93–106.

(33) Rahmelow, K.; Hubner, W. Secondary structure determination of proteins in aqueous solution by infrared spectroscopy: a comparison of multivariate data analysis methods. *Anal. Biochem.* **1996**, *241*, 5–13.

(34) Brauner, J. W.; Flach, C. R.; Mendeisohn, R. A quantitative reconstruction of the amide I contour in the IR spectra of globular proteins: from structure to spectrum. *J. Am. Chem. Soc.* **2005**, *127*, 100–109.

(35) Nemethy, G.; Scheraga, H. A. The structure of water and hydrophobic bonding in proteins. III. The thermodynamic properties of hydrophobic bonds in proteins. *J. Phys. Chem.* **1962**, *66*, 1773–1789.

(36) Timasheff, S. N. Thermodynamic of protein interactions [M]. In *Proteins of Biological Fluids*; Peeters, H., Ed.; Pergamon Press: Oxford, U.K., 1972; pp 511−519.

(37) Ross, P. D.; Subramanian, S. Thermodynamics of protein association reactions: forces contributing of stability. *Biochemistry* **1981**, *20*, 3096–3102.

(38) Peters, T. *All About Albumin*; Academic Press: New York, 1996.